

Supporting Information

Theoretical Insights into Effective Electron Transfer and Migration

Behavior towards CO₂ Reduction on the BiOBr (001) Surfaces

Xiaochao Zhang,^{*a} Tan Li,^b Xiushuai, Guan,^a Changming Zhang,^c Rui Li,^d Jinbo Xue,^e Jianxin Liu,^a Yawen Wang^a and Caimei Fan^{*a}

^aCollege of Chemistry and Chemical Engineering, Taiyuan University of Technology, Taiyuan 030024, P. R. China

^bSchool of Environment and Energy, South China University of Technology, Guangzhou 51006, P. R. China

^cCollege of Mining Engineering, Taiyuan University of Technology, Taiyuan 030024, P. R. China

^dCollege of Environmental Science and Engineering, Taiyuan University of Technology, Taiyuan 030024, P. R. China

^eKey Laboratory of Interface Science and Engineering in Advanced Materials (Taiyuan University of Technology), Taiyuan 030024, P.R. China.

Corresponding author:

Xiaochao Zhang, Caimei Fan, College of Chemistry and Chemical Engineering, Taiyuan University of Technology, Taiyuan 030024, PR China. **Tel.:** +86-15503477962; **Fax:** +86-351-6018554. **E-mail:** zhangxiaochao@tyut.edu.cn; fancm@163.com.

Acknowledgments

This work is financially supported by the National Natural Science Foundation of China (No. 21978196, 21978187, 22008167), China Postdoctoral Science Foundation (No. 2020M672825), Natural Science Foundation for Young Scientists of Shanxi Province (No. 201801D211008, 201901D211100, 201901D211058).

Surface formation energy

The surface energy is lower meaning that is more stable or more “bulklike”. And the molar chemical potential (μ) is known as partial molar free energy. The surface energy can be expressed as [1, 2]:

$$\sigma = \frac{1}{2A}(E^{slab} - nE^{bulk}) \dots\dots\dots(1)$$

The surface energy of BiOBr{001} can be expressed as:

$$\sigma_{001-O} = \frac{1}{2A}(E_{001-O}^{slab} - nE_{BiOBr}^{bulk} - 2\mu_O^{slab}) \dots\dots\dots(2)$$

$$\sigma_{001-O+H} = \frac{1}{2A}(E_{001-O+H}^{slab} - nE_{BiOBr}^{bulk} - 2\mu_O^{slab} - 4\mu_H^{slab}) \dots\dots\dots(2)$$

$$\sigma_{001-Bi} = \frac{1}{2A}[E_{001-Bi}^{slab} - nE_{BiOBr}^{bulk} - 2\mu_O^{slab} - 2\mu_{Bi}^{slab}] \dots\dots\dots(3)$$

$$\sigma_{001-Br} = \frac{1}{2A}(E_{001-Br}^{slab} - nE_{BiOBr}^{bulk}) \dots\dots\dots(4)$$

The chemical potential of O in the slab (μ_O^{slab}) must be less than the chemical potential of O in its bulk phases (μ_O), otherwise, the compound slab will be unstable and more favorable to form bulk phase. Therefore, the thermodynamic range of the O chemical potential is

$$\mu_O^{slab} \leq \mu_O \leq \frac{1}{2}\mu_{O_2} \dots\dots\dots(5)$$

$$\frac{1}{2}\Delta H_f \leq \Delta\mu_O \leq 0 \dots\dots\dots(6)$$

Where $\Delta\mu_O$ is defined as $\Delta\mu_O = \mu_O^{slab} - \mu_O^{mol}$.

Internal electric field (IEF) magnitude

The IEF magnitude (E_{IEF}) could be obtained through Eq.(7) [3]

$$E_{IEF} = \left(\frac{-2V_s \rho}{\varepsilon \varepsilon_0} \right)^{1/2} \dots\dots\dots(7)$$

Where, V_s is the surface voltage, ρ is the surface charge density, ε is the low-frequency dielectric constant, and ε_0 is the permittivity of free space. These meant that the E_{IEF} is mainly determined by the surface voltage and the charge density because ε and ε_0 are two constants.

A surface voltage (V_s) is usually the result of a surface or insulator charge or work function (Φ) difference and it is most commonly detected with a non-contacting probe [4]. Hence, no electric field exists between the sample and the probe making $V_s = \Phi$.

The charge density could be picked up through Eq. (8)

$$\rho = \left(\frac{F}{A} \right) \left[\left(\frac{10^{-2pH} - K_1 K_2}{10^{-2pH} + 10^{-2pH} K_1 + K_1 K_2} \right) N_T \right] \dots\dots\dots(8)$$

Where F is the Faraday constant, A is the total surface area, N_T is the total number of moles of surface sites, and K_1 and K_2 are the acid equilibrium constants.

From the above, with no external electric field, the E_{IEF} was in direct proportion to work function (Φ) and inversely proportional to the surface area value ($SA=A/N_T$), as Eq. (9) shown:

$$E_{IEF} \propto \frac{\Phi}{A} \dots\dots\dots(9)$$

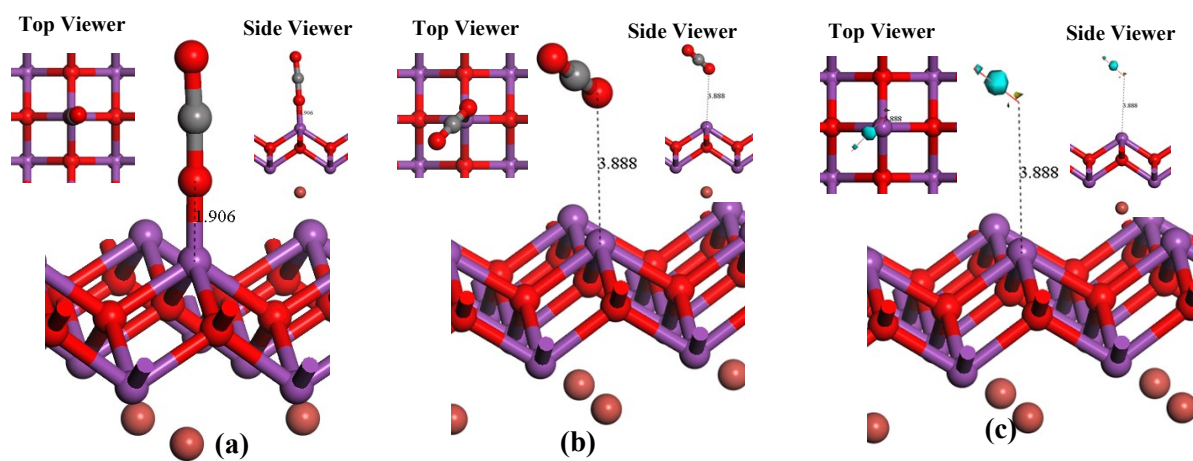


Figure S1 The structure for the O atoms of CO₂ adsorption on BiU adsorption site of BiOBr (001Bi) surface: (a) before optimization, (b) after optimization and (c) electron difference density.

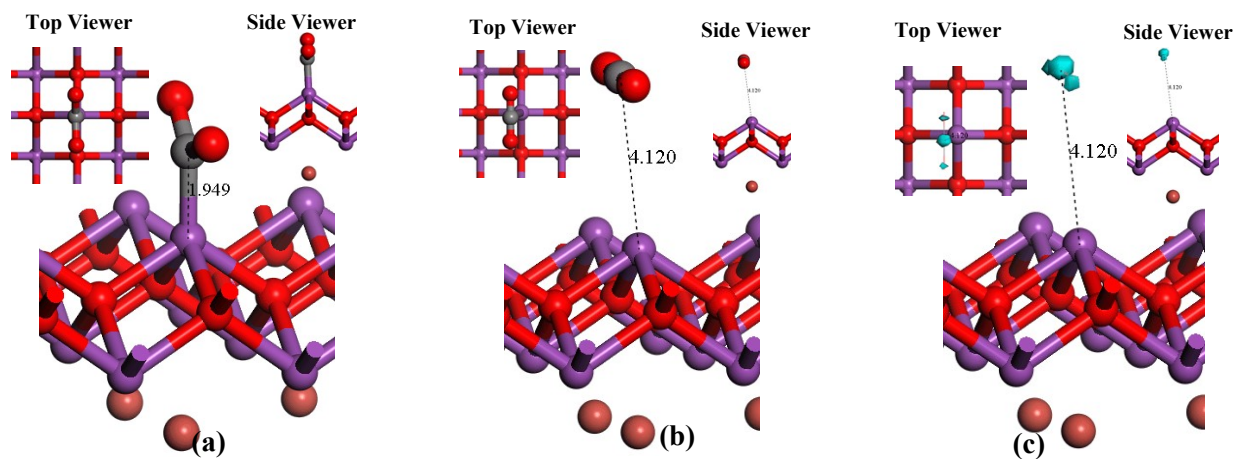


Figure S2 The structure for the C atoms of CO₂ adsorption on BiOBr (001Bi) surface: (a) before optimization, (b) after optimization and (c) electron difference density.

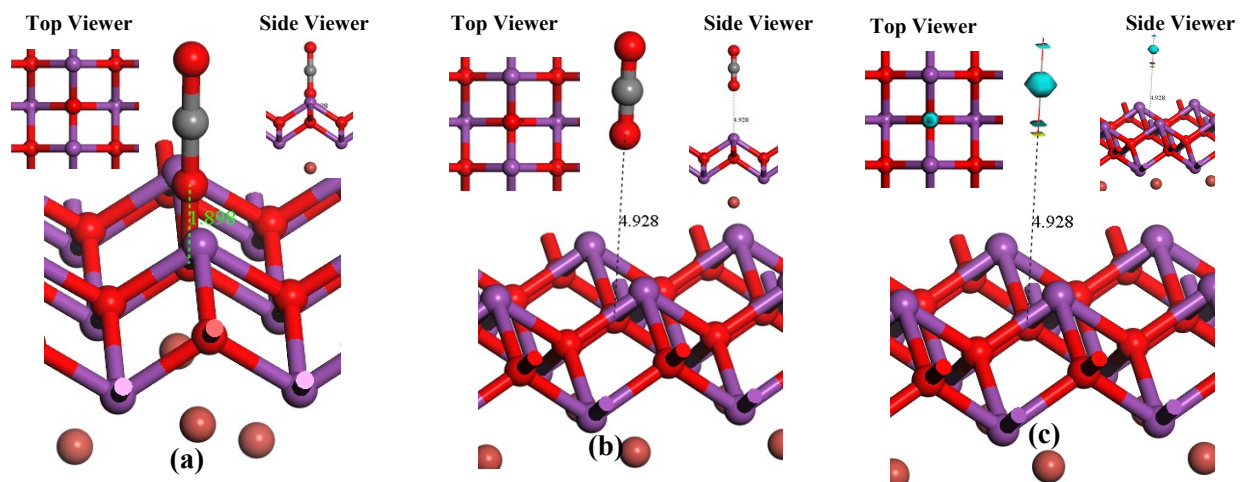


Figure S3 The structure for the O atoms of CO₂ adsorption on O adsorption site of BiOBr (001Bi) surface: (a) before optimization, (b) after optimization and (c) electron difference density.

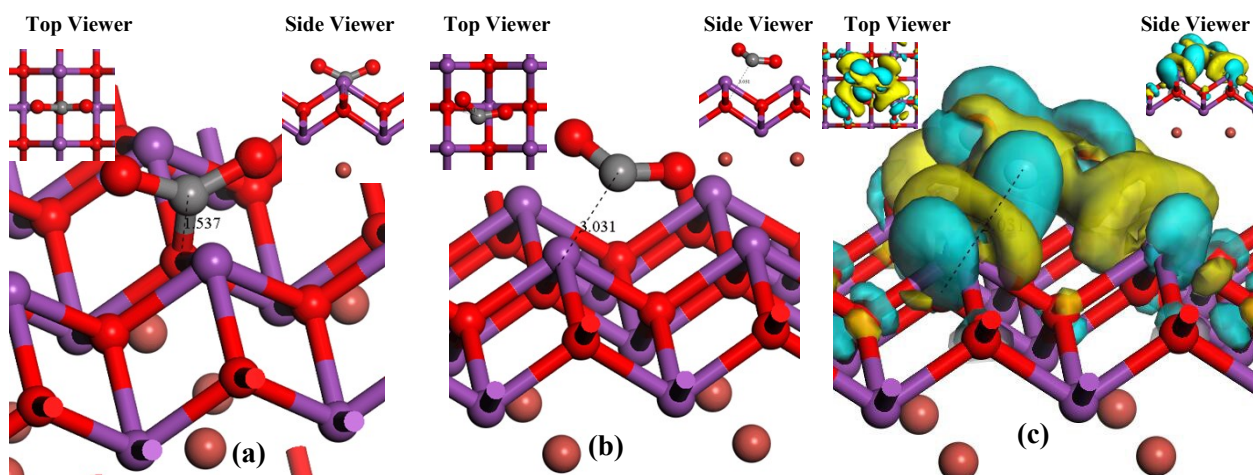


Figure S4 The structure for the C atoms of CO₂ adsorption on O adsorption site of BiOBr (001Bi) surface: (a) before optimization, (b) after optimization and (c) electron difference density.

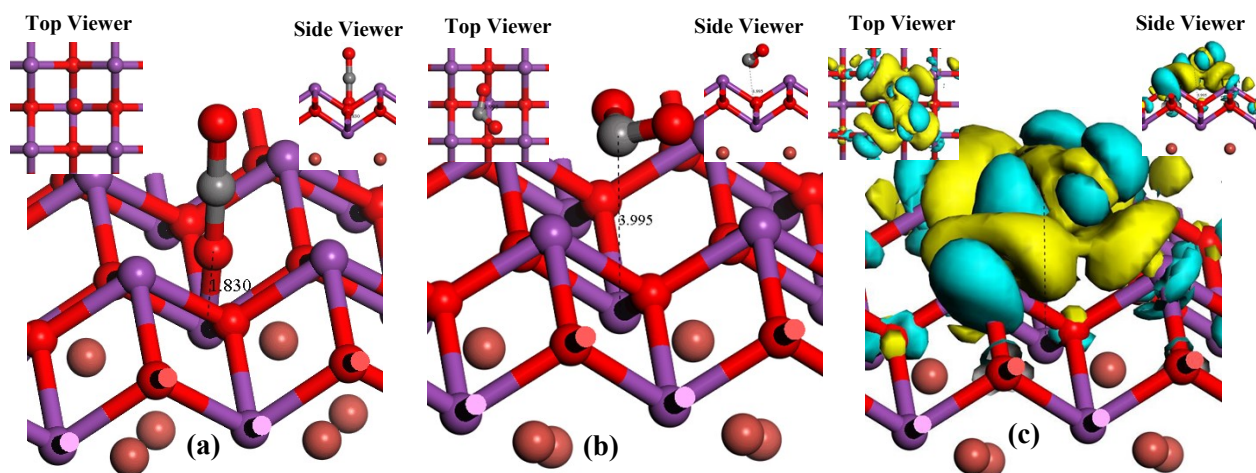


Figure S5 The structure for the O atoms of CO₂ adsorption on BiD adsorption site of BiOBr (001Bi) surface: (a) before optimization, (b) after optimization and (c) electron difference density.

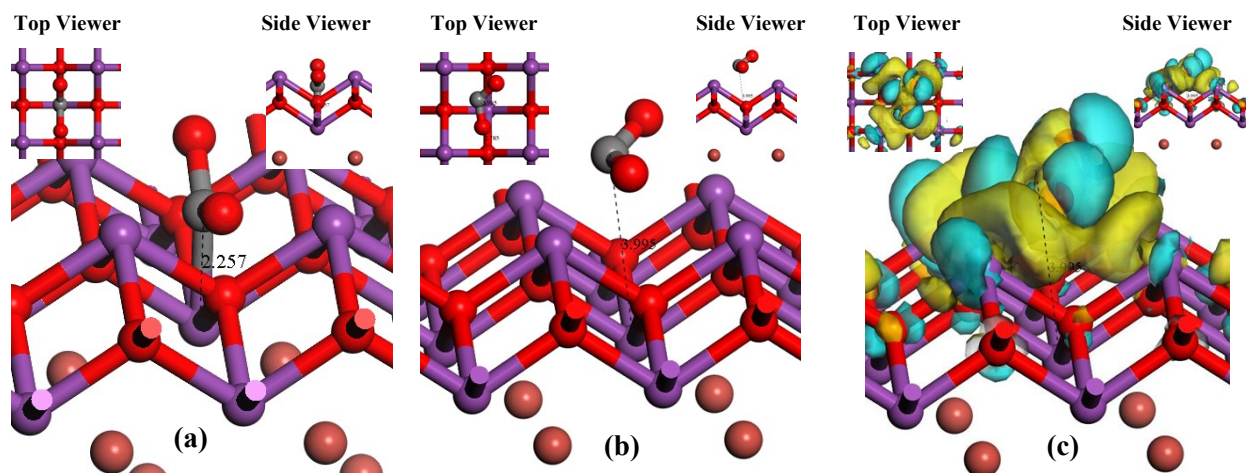


Figure S6 The structure for the C atoms of CO₂ adsorption on BiD adsorption site of BiOBr (001Bi) surface: (a) before optimization, (b) after optimization and (c) electron difference density.

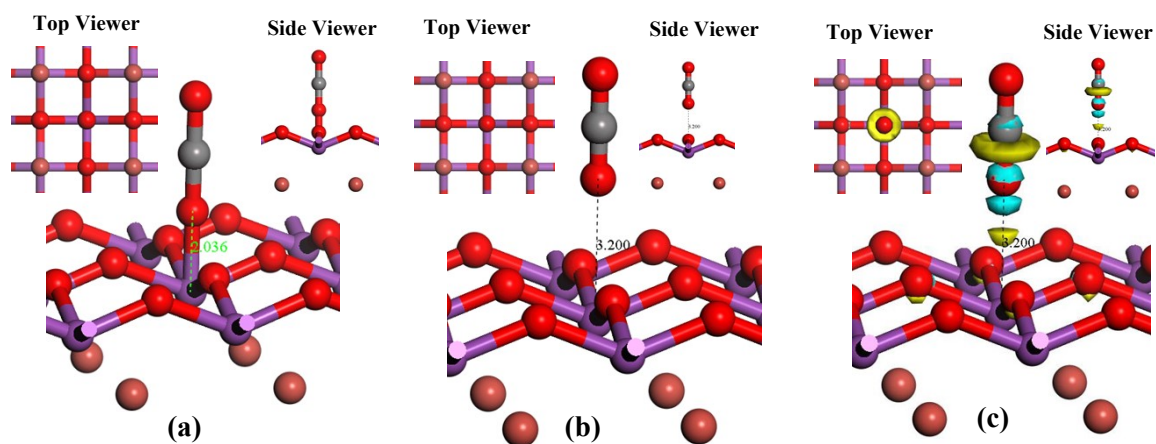


Figure S7 The structure for the O atoms of CO₂ adsorption on Bi adsorption site of BiOBr (001) surface: (a) before optimization, (b) after optimization and (c) electron difference density.

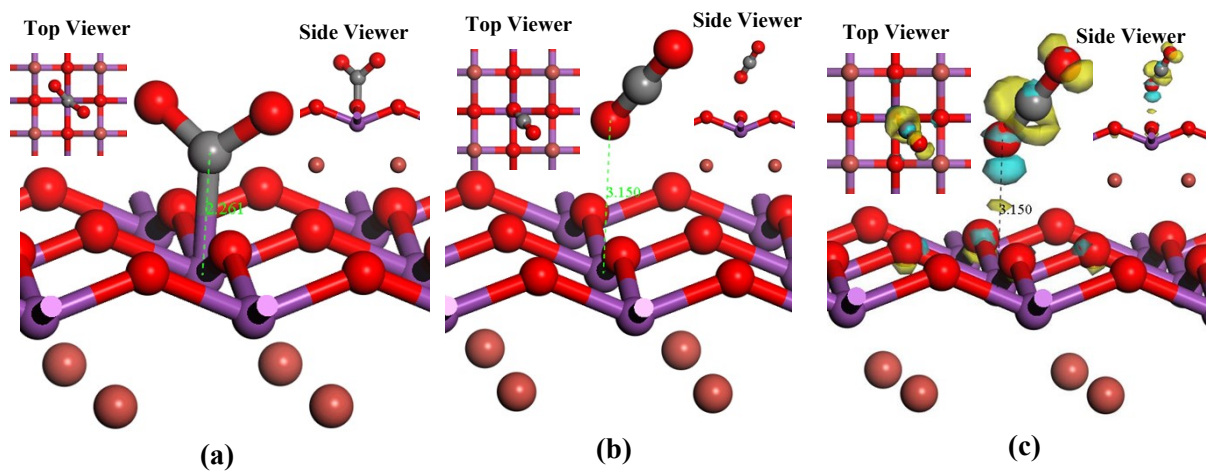


Figure S8 The structure for the C atoms of CO₂ adsorption on Bi adsorption site of BiOBr (001O) surface: (a) before optimization, (b) after optimization and (c) electron difference density.

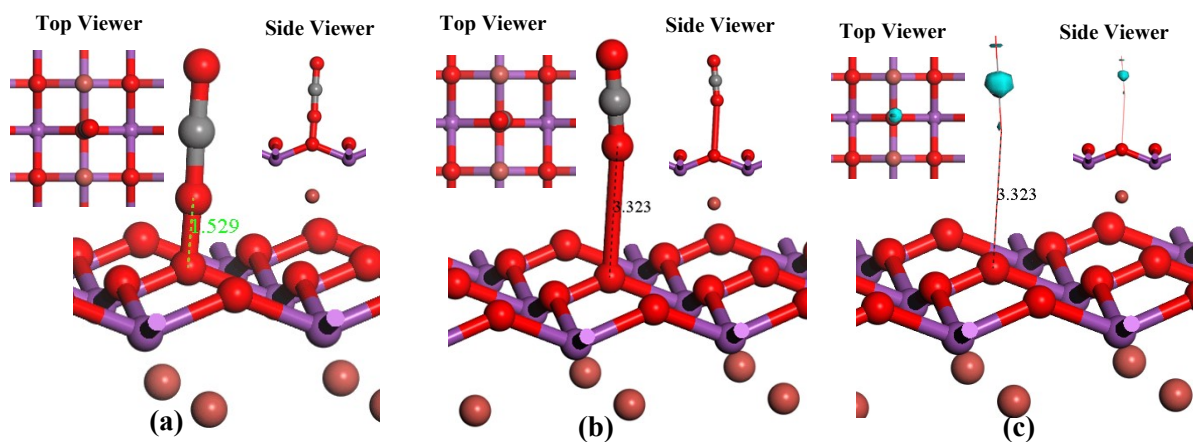


Figure S9 The structure for the O atoms of CO_2 adsorption on O adsorption site of BiOBr (0010) surface: (a) before optimization, (b) after optimization and (c) electron difference density.

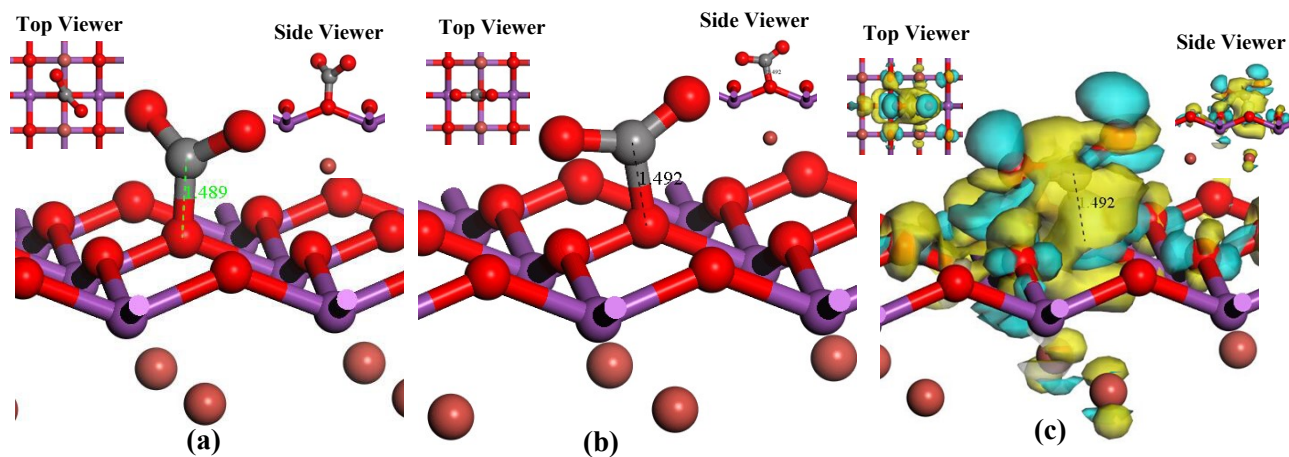


Figure S10 The structure for the C atoms of CO_2 adsorption on O adsorption site of BiOBr (0010) surface: (a) before optimization, (b) after optimization and (c) electron difference density.

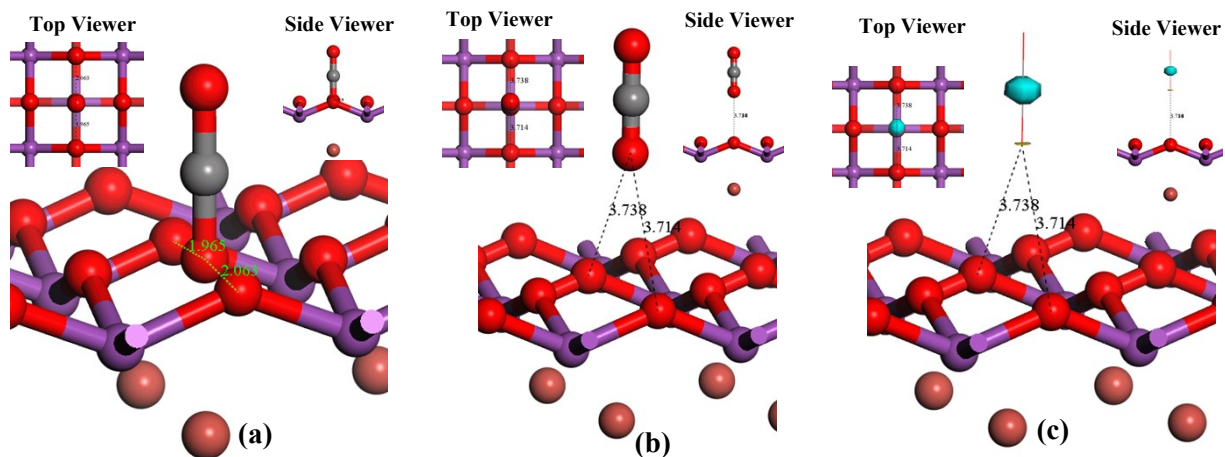


Figure S11 The structure for the O atoms of CO₂ adsorption on Br adsorption site of BiOBr (0010) surface: (a) before optimization, (b) after optimization and (c) electron difference density.

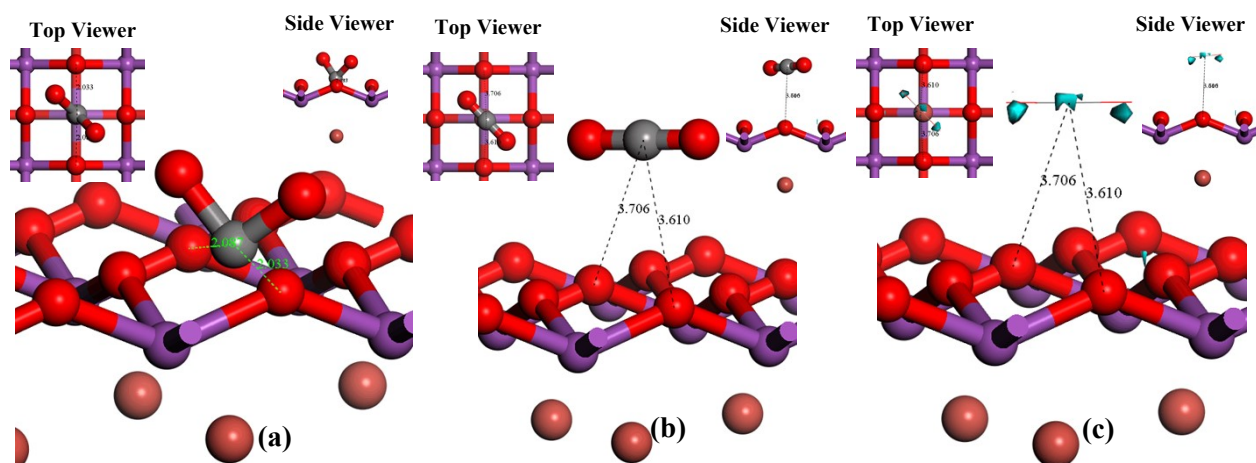


Figure S12 The structure for the C atoms of CO_2 adsorption on Br adsorption site of BiOBr (0010) surface: (a) before optimization, (b) after optimization and (c) electron difference density.

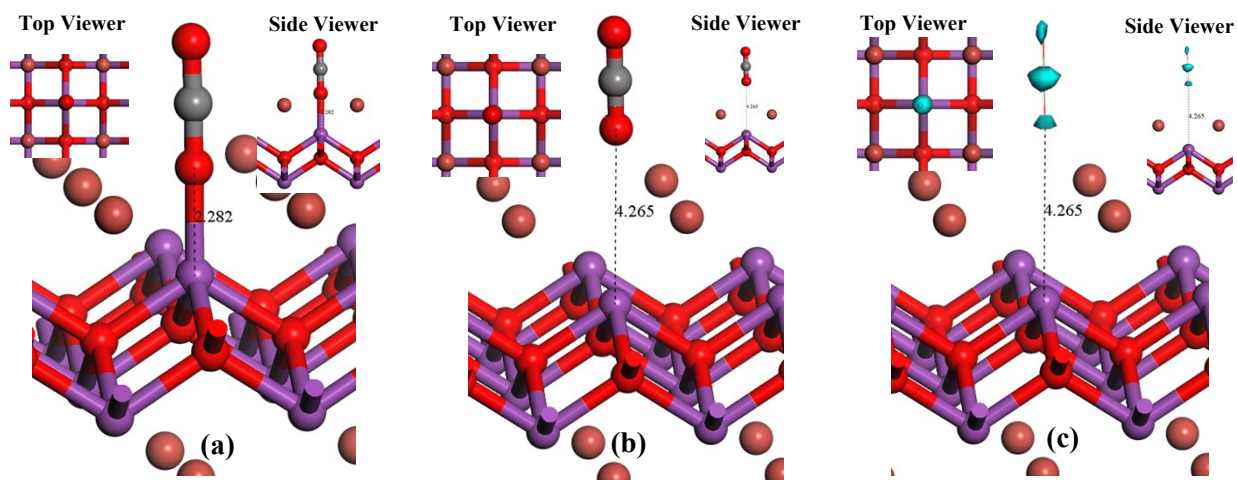


Figure S13 The structure for the O atoms of CO₂ adsorption on Bi adsorption site of BiOBr (001Br) surface: (a) before optimization, (b) after optimization and (c) electron difference density.

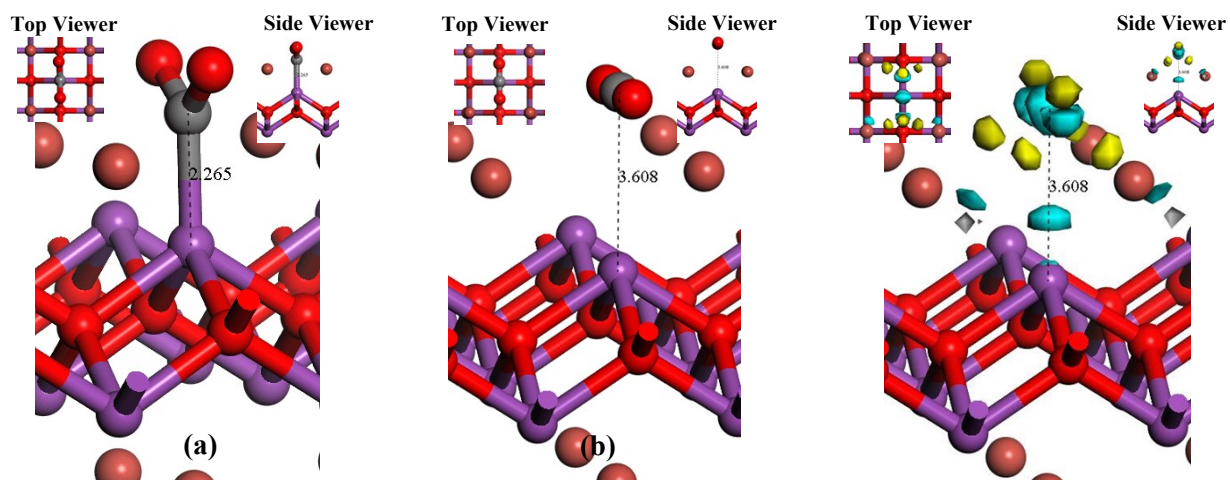


Figure S14 The structure for the C atoms of CO₂ adsorption on Bi adsorption site of BiOBr (001Br) surface: (a) before optimization, (b) after optimization and (c) electron difference density.

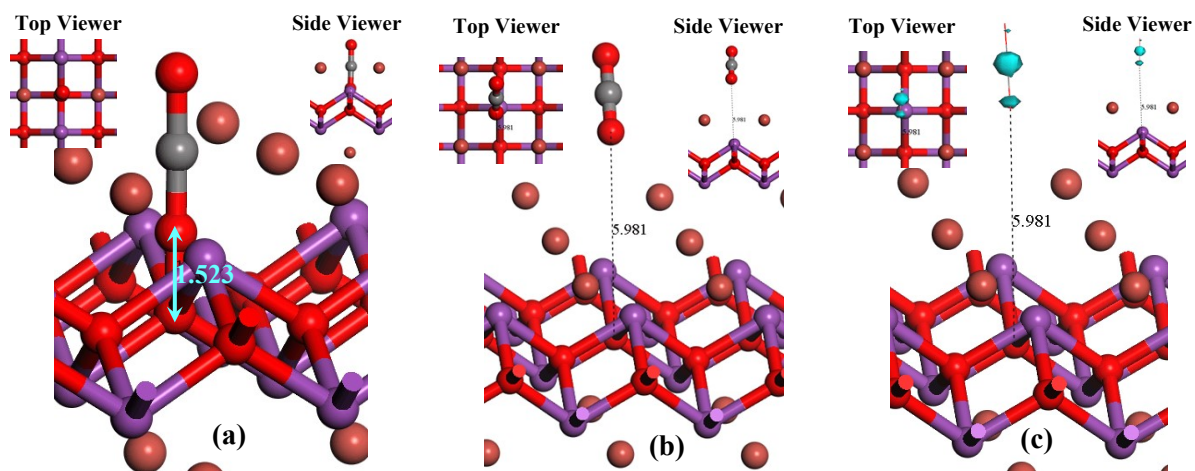


Figure S15 The structure for the O atoms of CO₂ adsorption on O adsorption site of BiOBr (001Br) surface: (a) before optimization, (b) after optimization and (c) electron difference density.

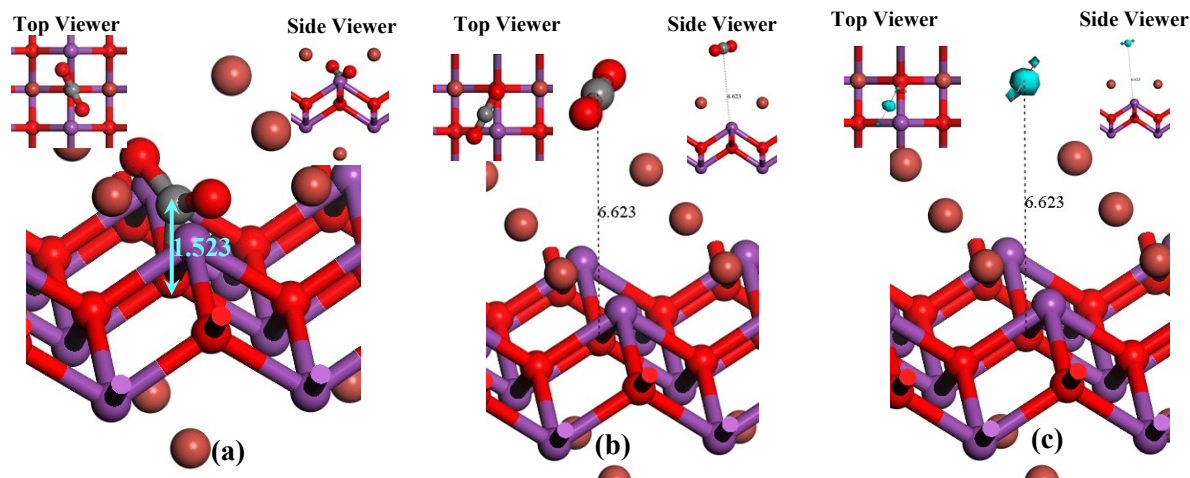


Figure S16 The structure for the C atoms of CO₂ adsorption on O adsorption site of BiOBr (001Br) surface: (a) before optimization, (b) after optimization and (c) electron difference density.

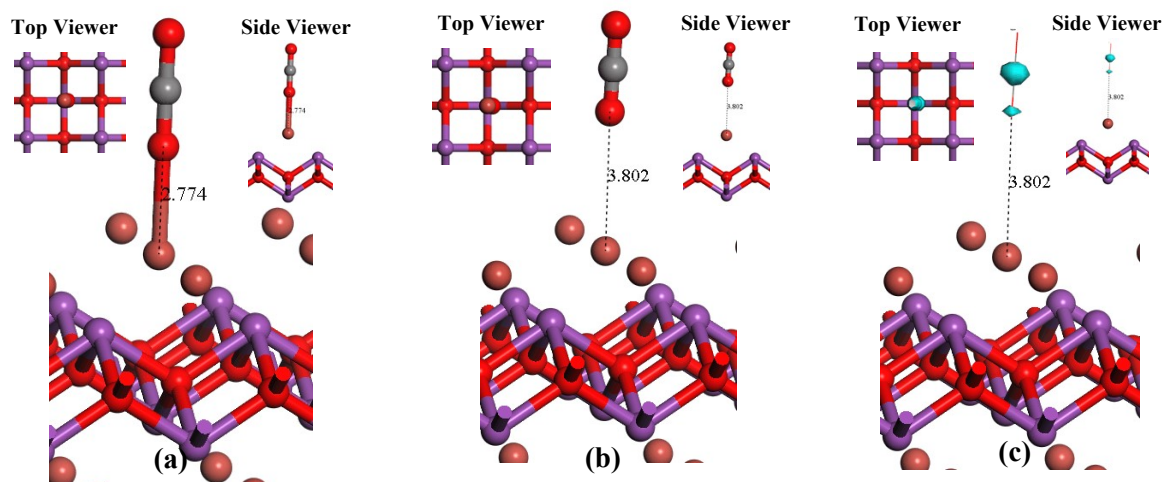


Figure S17 The structure for the O atoms of CO₂ adsorption on Br adsorption site of BiOBr (001Br) surface: (a) before optimization, (b) after optimization and (c) electron difference density.

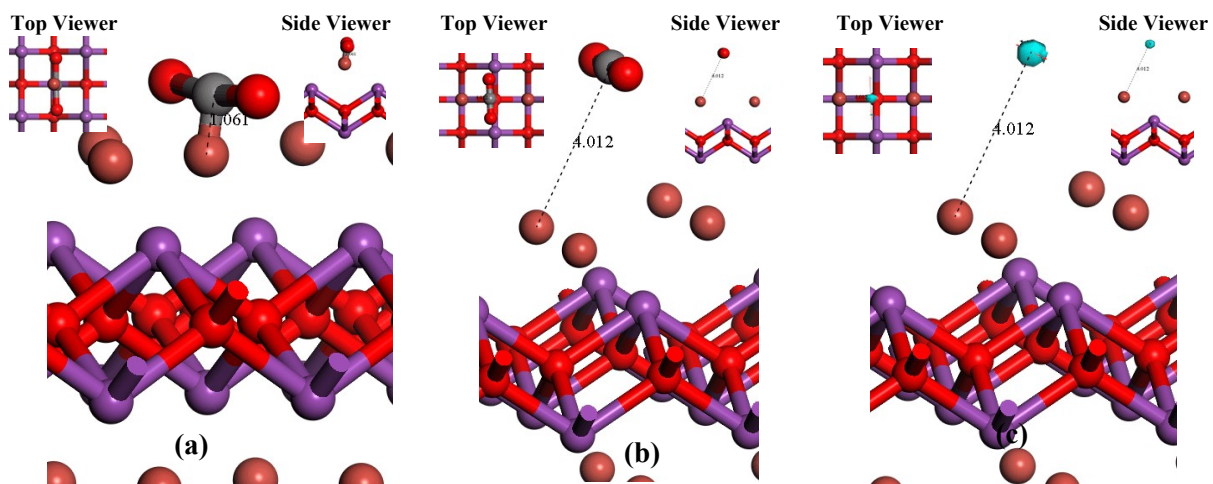


Figure S18 The structure for the C atoms of CO₂ adsorption on Br adsorption site of BiOBr (001Br) surface: (a) before optimization, (b) after optimization and (c) electron difference density.

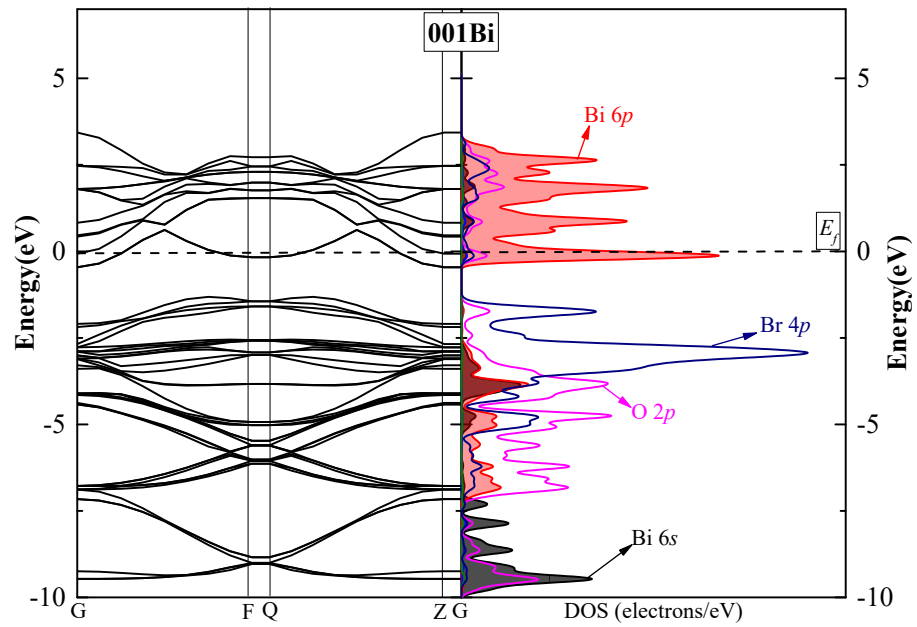


Figure S19 Band structures and density of states for BiOBr (001Bi) surface.

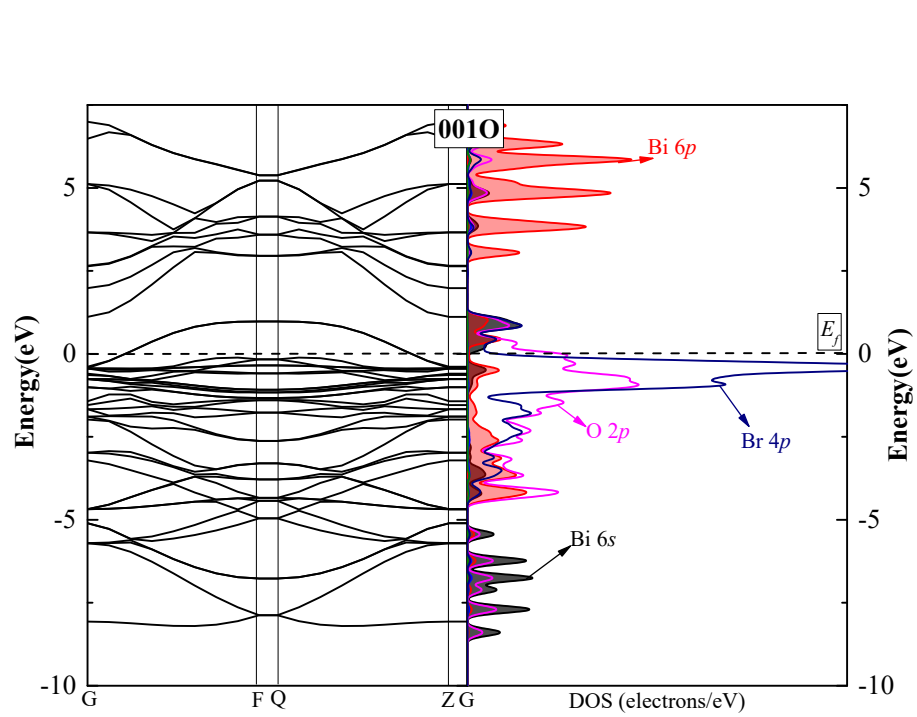


Figure S20 Band structures and density of states for BiOBr (0010) surface.

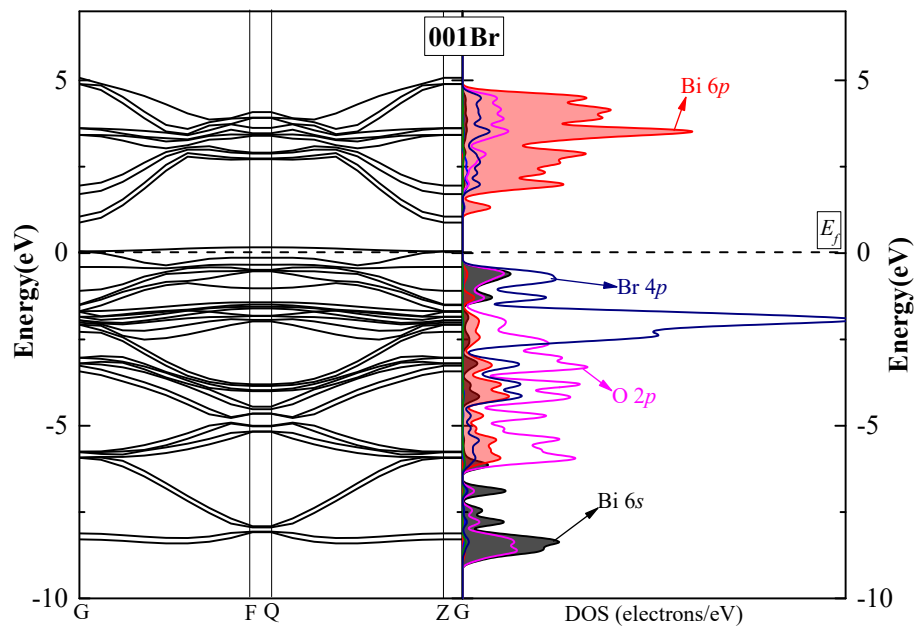


Figure S21 Band structures and density of states for BiOBr (001Br) surface.

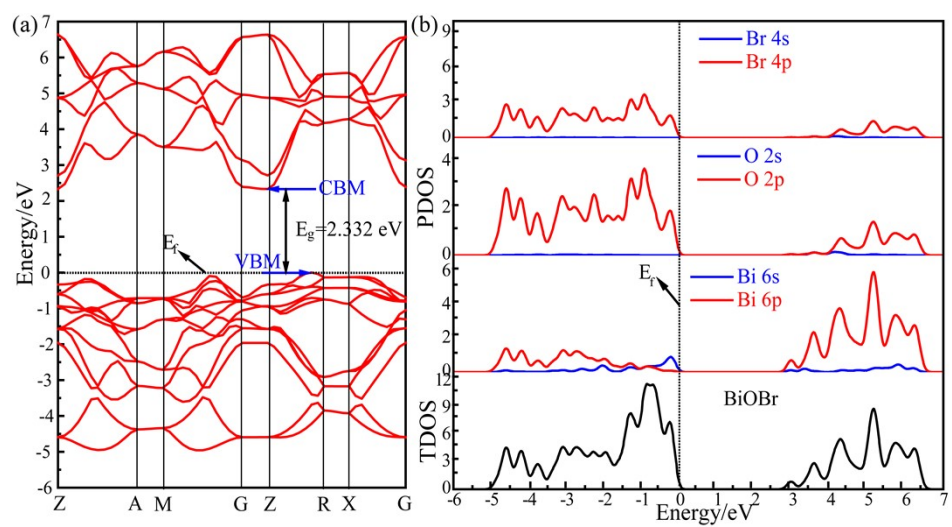


Figure S22 Band structure and density of states for bulk BiOBr.

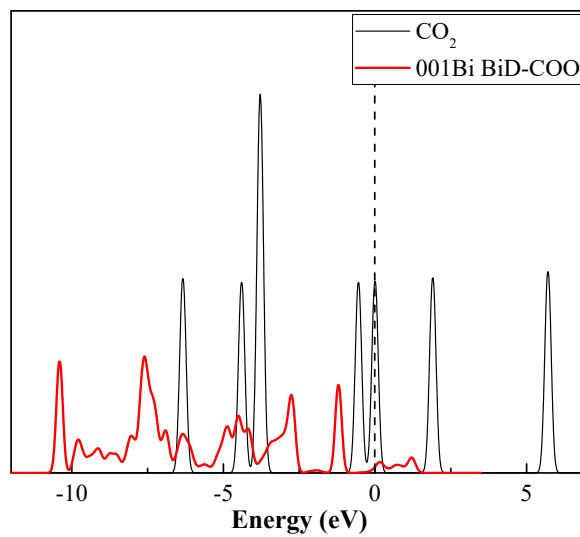


Figure S23 The LDOS of CO₂ before and after chemisorption on BiD site of BiOBr (001) surface with Bi-termination.

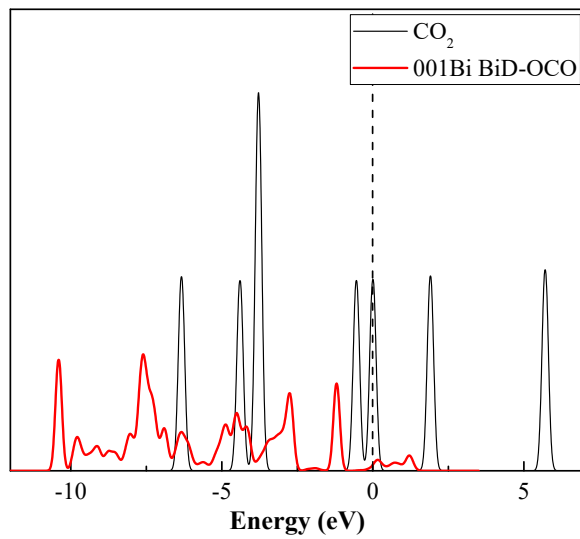


Figure S24 The LDOS of CO₂ before and after chemisorption on BiD site of BiOBr (001) surface with Bi-termination.

Reference

- [1] D.S. Sholl, J.A. Steckel. Hoboken, New Jersey: *John Wiley & Sons, Inc.*; 2009. 82-112.
- [2] K. Zhao, L.Z. Zhang, J.J. Wang, Q.X. Li, W.W. He, J.J. Yin. *J. Am. Chem. Soc.*, 2013, **135**, 15750-15753.
- [3] J. Li, L.J. Cai, J. Shang, Y. Yu, L.Z. Zhang. *Adv. Mater.*, 2016, **28**, 4059-4064.
- [4] D.K. Schroder. *Meas. Sci. Technol.*, 2001, **12**, R16-R31.